Malachite Green Dye Removal from Aqueous Solutions Using Invader *Centaurea Solstitialis* Plant and Optimization by Response Surface Method: Kinetic, Isotherm, and Thermodynamic Study

Mohammed Saleh[1*], Mutlu Yalvaç[2], Hüdaverdi Arslan[3], and Melis Gün[4]

[1] Mohammed Saleh: PhD. Student, Environmental Engineering Department, Mersin University. Mersin, Turkey (ORCID: 0000-0002-3145-4457)
[2] Mutlu Yalvaç: PhD, Environmental Engineering Department, Mersin University, Mersin, Turkey (ORCID: 0000-0002-1281-5712)
[3] Hüdaverdi Arslan: PhD, Environmental Engineering Department, Mersin University, Mersin, Turkey (ORCID: 0000-0002-3053-6944)
[4] Melis Gün: BSc. Student, Environmental Engineering Department, Mersin University. Mersin, Turkey (ORCID: 0000-0001-7982-6013)

Abstract

Invasive plants reduce the yield by inhibiting the development of agricultural products. In this study, invasive (CS) plant which is agricultural waste was used as adsorbent for removal of Malachite Green (MG) from aqueous solution. The adsorbent - adsorbate relationship was examined by the spectrophotometric method and Fourier transform infrared (FTIR). The surface morphology was determined by scanning electron microscope (SEM). CS surface area was measured by Brunauer, the Emmett and Teller (BET) analysis. The experiments were designed and modeled by RSM. The correlation factor of the developed model was 0.984. The capacity of 90.816 mg.g^{-1} was achieved when MG solution with concentration of 312.5 mg.L^{-1} was adsorbed onto 0.325 g CS for 75 min at a pH of 7.5. In this work the shaking velocity and the adsorbent size were 150 rpm and 30 mesh respectively. Langmuir, Freundlich, Temkin, and Dubinin-Radushkevich (D-R) isotherms were studied. Temkin isotherm had the highest R^2 of 0.997. The kinetics models of the adsorption process were investigated and fitted with pseudo-second-order kinetic (R^2 = 0.9982). The intraparticle diffusion model reflected the involved two steps; the first comprehended the boundary diffusion layer, while the second introduced the intraparticle diffusion effects. The adsorption was found to be endothermic with a Gibbs free energy of -4.47 KJ.mol^{-1}. It was noted that the adsorption process was irreversible with a max percentage of desorption process of 2.16%. Column experiments were conducted to realize the adsorption process. The efficiency of the column reached 99.5% after 40 min and stilled constant. As a result, CS has shown a potential for MG removal from aqueous solution.

Keywords: Malachite Green; *Centaurea solstitialis*, Adsorption process; Response Surface Method.

İstilacı *Centaurea Solstitialis* Bitkisi Kullanılarak Sulu Çözeltilerden Malahit Yeşil Boya Giderimi ve Tepki Yüzey Yöntemi ile Optimizasyon: Kinetik, İzoterm ve Termodinamik Çalışma

Öz

İstilacı bitkiler, tarım ürünlerinin gelişimini engelleyerek ürün verimini azaltmaktadır. Bu çalışmada, sentetik bir boya olan Malachite Green (MG)'nin sulu çözeltiden uzaklaştırılmasında tarımsal atık olan istilacı *Centaurea Solstitialis* (CS) bitkisi adsorban olarak kullanılmıştır. Adsorbent - adsorbate ilişkisi, spektrofotometrik yöntem ve Fourier dönüşüm infrared (FTIR) ile incelenmiştir. Yüzey morfolojisi taramalı elektron mikroskobu (SEM) ile belirlenmiştir. CS yüzey alanı Brunauer, Emmett ve Teller (BET) analizi ile

---

*Mohammed Saleh: PhD. Student, Environmental Engineering Department, Mersin University. Mersin, Turkey (ORCID: 0000-0002-3145-4457), muh.saleh89@gmail.com

ölçülmüştür. Deney tasarımı ve modellemesinde RSM kullanılmış ve korelasyon faktörü 0,984 olarak bulunmuştur. Optimum çalışma koşulu olan 312.5 mg.L^{-1}MG içeren çözeltiye (pH=7.5) 0.325 g CS (30 mesh) koyularak 150 rpm'de 75 dakika çalkalanmıştır. Çalışmada CS tanecik boyutu 30 mesh ve çalkalama hızı 150 rpm sabit tutulmuştur. Optimum çalışma koşullarında CS'nin maksimum adsorpsiyon kapasitesi 90.816 mg.g^{-1} bulunmuştur. Sonuçlar Langmuir, Freundlich, Temkin ve Dubinin-Radushkevich (D-R) izotermleri ile değerlendirilmiştir. Sonuç olarak adsorpsiyon işleminin Temkin izotermine (0,997 R^2) uyan yalancı ikinci dereceden (R^2 = 0.9982) bir kinetik reaksiyon olduğu bulunmuştur. İntrapartikül difüzyon modeli, sırasıyla sınır difüzyon tabakası ve partikül içi difüzyon etkilerini göstermiştir. Adsorpsiyonun -4,47 KJ.mol^{-1} Gibbs serbest enerjisi ile endotermik olduğu bulunmuştur. Desorpsiyon çalışmasında maksimum %2.16'lık bir verim elde edilmiştir. Bu sonuç CS üzerine adsorbe olan MG'nin tekrar suya karışma ihtimalinin düşük olduğunu göstermektedir. Daha sonra kolon çalışmalarına geçilmiştir. Kolonun verimliliği, 40. dakikada % 99.5'e ulaşmış ve bundan sonra sabit kalmıştır. Sonuç olarak, CS'nin, sulu çözeltiden MG gideriminde etkili bir adsorbent olduğu bulunmuştur.

Anahtar Kelimeler: Malahit Yeşili, *Centaurea solstitialis*, Adsorpsiyon işlemi, Tepki Yüzey Yöntemi.

1. Introduction

Dyes are material used for coloring purposes. It can be synthetic or natural (Saxena and Raja 2014). Although Synthetic dyes are more economically and beneficiary than natural, the natural dyes are more favorable environmentally. Synthetic dyes may affect human (Bapat and Jaspal 2016) and the environment seriously (Robinson et al. 2001). Paper, hair color, food, plastic, and textile industries are examples for the dyes uses (Mittal et al. 2010). Dyes manufacturing has increased rapidly, with a production of 555 million tons/year for over 1000,000 types. Most of these types are related to water pollution (Mittal et al. 2009; Saravanan et al. 2016). In Turkey, The productions of dyes have reached 903 thousand tons for 2018 (Paint Industry in Turkey and the World 2018).

The green crystal powder dye named Malachite Green (MG) is soluble in water and belongs to tri phenyl methane category (Raval et al. 2016). It is not used in dying only, but it used as antiseptic, antiphrastic, antibacterial and antifungal. It can cause nervous system, skin, eye, kidney, and heart damages. So a proper treatment should be chosen to protect the human and the environment (Raval et al. 2017; Khan et al. 2011).

Several treatment methods were utilized to remove MG from aqueous solution. Levin et al. (2004) study the biodegradation of MG by white root fungi. The Malachite Green decolorization by Algal species was tested (Abd-El-Kareem and Taha, 2012). Man et al. (2012) examined the thermolysis - coagulation-flocculation process for MG removal. Chemical methods like ozonation and Fenton's reagent showed capabilities in treating MG (Zhou et al. 2013; Bai et al. 2013; Chen et al. 2002). Photocatalytic, photo-oxidative, and solar degradations were also examined (Hasanat et al. 2003; Yang et al. 2005; Aliyan et al. 2013; Bojinova and Dushkin 2011; Modirshahla and Behnajady 2006; Pirsaheb et al. 2015). Efficiency, engineering perspective, value, and effectiveness still have limited on the above techniques (Raval et al. 2017).

The adsorption process is the removing of the particles employing the transfer of mass from the liquid phase onto the solid phase (Crittenden et al. 2012). The process of adsorption is more favorable than the chemical methods, it is simpler and more flexible (Tobías et al. 2018). In addition to that, the adsorption process does not generate any sludge as in the biological process (Khamparia and Jaspal 2017). For these reasons, the adsorption process became the most frequent process.Activated carbon had been used widely as an adsorbent. Because of its cost, researchers attitude to use low-cost adsorbents (Gupta 2009; Salleh et al. 2011).

Time, pH, the concentration of dye, and adsorbent mass affect the adsorption process (Saleh et al. 2019). The relation between each factor and the adsorption process should be predicted. In the past, the effect of each factor was studied individually at the time (Gadekar and Ahammed 2019). Researchers had developed a collection of statistical and mathematical techniques called Response surface method (RSM) (Bezerraa et al. 2008). RSM had solved the problem by creating a model predicting the relation between them.

Many crops are cultivated in Mersin due to its location in the Mediterranean region, climate, soil structure, and geographical features. Due to the same reasons, there are many invasive plant species grows around the crops. These plants are no useful use. They are removed from agricultural areas and disposed of as waste. One of these is *Centaurea solstitialis* (CS). Farmers try to dispose of it by chemical and physical techniques. This study aims to investigate the ability of removal of MG from aqueous solution by CS plants and optimize the process by using RSM.

2. Material and Method

2.1. Adsorbent Preparation

CS was collected from the farmland near Mersin. It was washed enough by distilled water to remove clay and other solids. After that, it was dried at 105 °C using Heraeus oven for 24 h. The dried adsorbent was grinded by ISOLAB blender and sieved at 30 mesh without any further treatment. It was prepared in adequate quantity to avoid any unexpected faults. Figure 1 shows the CS.

Figure 1. The collected CS

2.2. Dye Preparation

The organic chloride salt dye named Malachite green was purchased from Sigma-Aldrich. The cationic MG dye has a chemical formula of $C_{23}H_{25}ClN_2$ (Figure2) and a molecular weight of 346.9 g. mol^{-1}. A stock solution with 1000 ppm was prepared and kept till the end of experiments. The stock was used to prepare the proposed concentrations. The desired pHs were modified using 0.1 M sodium hydroxide (NaOH) and 0.1 M hydrochloric acid (HCl). The concentration changes were obtained using UV-visible spectroscopy at a wavelength of 618 nm (Raval et al. 2017).
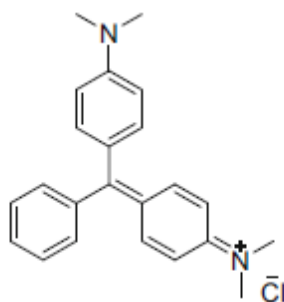

Figure 2. Chemical structure of MG dye (Raval et al. 2017).

2.3. Adsorbent Characterization

Adsorbent and dye weights were measured by a precision scale (Uhaus Corp Adventure); the orbital shaker (Stuart Biolab) was used to mix the solution; pH meter (ISOLAB) was used to measure the Hydrogen ions concentration in the solution. The concentrations of dyes were measured using UV-Visible spectrophotometer (T 90); Fourier transform infrared spectrophotometer was utilized to determine the CS infrared spectra. In addition to that, the surface area and surface morphology were identified by BET analysis and scanning electron microscope (SEM) (Gemini Zeiss Supra 55).

2.4. Batch Study

In the batch study, the common affecting factors such as pH, the mass of adsorbent, the initial concentration and the contact time were investigated (Gupta et al. 2015). The volume of solution was 100 mL for all the experiment. Samples were drained into the 250 mL flask to avoid any missing in the solution quantity. The efficiency and the adsorbent capacity (q_e) were calculated using equation 1 and equation 2, respectively (Bagheri et al. 2019):

$$Efficiency = (C_i - C_f)/C_i \times 100\% \qquad \text{Equation 1}$$

$$q_e = (C_i - C_f) \times V/m \qquad \text{Equation 2}$$

Where, C_i is the MG initial concentration (mg.L^{-1}), C_f is the final concentration (mg.L^{-1}); respectively. V is the solution volume (L); m is the CS mass (g).

To calculate the recovery percentage, desorption experiments were conducted by soaking the exhausted adsorbent in 0.1M sodium hydroxide (NaOH) and 0.1M hydrochloric acid (HCl). The solutions were waved at 150 rpm. And the recovery percentage was calculated as shown in equation 3.

$$\% \ Recovery = Amount \ of \ dye \ desorbed \ / \ Amount \ of \ dye \ adsorbed \times 100\%$$ Equation 3

2.5. Isotherms

To clarify the affinity between the adsorbate and the adsorbent, adsorption isotherms were performed by exposing 200 mg.L^{-1} of MG in 100 mL volume to various dosage of CS. Langmuir (Langmuir 1918), Freundlich (Freundlich 1906), Tempkin (Tempkin and Pyzhev 1940), and Dubinin-Radushkevich (D-R) (Dabrowski 2001) isotherms were studied. Langmuir describes the equilibrium between the solid surface and the liquid. In this case, it describes the equilibrium between the surface of CS and the MG. The formation of MG monolayer on the outer surface of the adsorbent CS was quantified. Equation 4 shows Langmuir isotherm linear form (Langmuir 1918). Freundlich isotherm (Equation 5) which is proposed originally as an empirical formula, describes the heterogonous of the CS (Freundlich 1906). Temkin isotherm describes the adsorption heat. It assumes that the heat of the adsorbent will decrease linearly for all molecules in the layer as shown in Equation 6 (Aharoni and Ungarish 1977). The distribution of Gaussian energy onto a heterogeneous surface was described by Dubinin-Radushkevich (D-R) as shown in Equation 7 (Gunay et al. 2007). The linear form of the used isotherm represented in Table 1.

Table 1.Shows the linear form of the used isotherm.

Isotherm	Linear form	Equation	Reference
Langmuir	$C_A/q_A = 1/(b_A q_m) + C_A/q_m$	Equation 4	(Langmuir 1918)
Freundlich	$Log(q_A) = log(K_A) + (1/n)log(C_A)$	Equation 5	(Freundlich 1906)
Temkin	$q_A = RT/b_T LnA_T + RT/b_T lnC_A$	Equation 6	(Tempkin and Pyzhev 1940)
Dubinin-Radushkevich (D-R)	$Lnq_A = Lnq_s - K_{ad}[RTLn \ (1 + 1/C_A)]^2$	Equation 7	(Dabrowski 2001)

- C_A is the concentration of adsorbate A at the equilibrium (mg.L^{-1})

- b_A is the Langmuir constant for the adsorbate A (L.mg^{-1})

- Q_M maximum adsorbent capacity at saturation (mg.g^{-1})

- K_A is the Freundlich adsorption capacity parameter (mg.g^{-1}) (L.mg^{-1}) $^{1/n}$

- $1/n$ is the intensity parameter

- R is the universal gas constant (8.314J K^{-1} M^{-1})

- T is the absolute temperature

- b_T is Temkin isotherm constant

- A_T is the binding constant (L.g^{-1})

- q_s is the theoretical saturation capacity (mg.g^{-1})

- K_{ad} is the isotherm constant (mol^2.kj^{-2})

- T is the absolute temperature

2.6. Adsorption Kinetics

Kinetic studies were performed by analysing the sample over time. The sampling process continued until the concentration of the sample became closer. The samples were fitted by Lagergren's pseudo first order model (Pal and Pal, 2017) and pseudo second-order model (Robati, 2013) as shown in Equation 8 and 9 respectively.

$$Log(q_e - q_t) = Logq_e - (k1/2.303)t$$ Equation 8

$$t/q_t = 1/(K_2 q_e^2) + (1/q_e)t$$ Equation 9

Where qe and qt are the adsorbent (CS) capacity at the equilibrium and at time (t) respectively (mg.g^{-1}). k_1 is Lagergren's constant (min^{-1}), k_2 is the constant of second order rate (mg.g^{-1}.min^{-1}). In addition to that, intraparticle diffusion model was plotted to as shown in equation 10 (Belhouchat and Zaghouane-Boudiaf 2017).

$$q_t = K_i t^{0.5} + C$$ Equation 10

Where ki is the intraparticle diffusion rate constant (mg.g.min$^{-1/2}$), C is a constant related to thickness of the boundary layer

2.7. Adsorption Thermodynamics

The feasibility, spontaneity, and randomness of the adsorption process can be identified by thermodynamics concepts. It realizes the relationship between the adsorbent and the adsorbate. Thermodynamics parameters were calculated as shown in Equation 11-13.

$$\Delta G = -RTLnb \hspace{4cm} \text{Equation 11}$$

$$\Delta H = -R(T_2T_i/(T_2 - T_1))Ln(b_2/b_1) \hspace{3cm} \text{Equation 12}$$

$$\Delta s = (\Delta H - \Delta G)/T \hspace{4cm} \text{Equation 13}$$

Where ΔG is the Gibbs free energy changes; ΔH and ΔS is the Enthalpy and Entropy respectively; b is the Langmuir constant. R is the universal gas constant (8.314 J.K^{-1}.M^{-1}) and T refers to temperature in Kelvin.

2.8. Response Surface Method (RSM)

Response surface method was applied the same as explained in the previous study by Saleh et al. (2019). Time, pH, the concentration of MG, and the mass of CS effects were modelled by Design expert v11 program. The factors ranges were determined and entered into the model (Saleh et al. 2019). Table 2 shows the factors and level of interest.

Table 2. Factors and level of interest

Variables	Unit	Factors	Low	High
pH	-	A	4.5	7.5
Time	Min	B	33.75	91.25
CS mass	G	C	0.325	0.775
MG concentration	mg L^{-1}	D	137.5	312.5

2.9. Column Study

Column experiment is an important issue to decide if the adsorbent can be realized or not. The experiment was conducted in 25 cm long column with an internal diameter of 1cm. The adsorbent was inserted into the column for a height of 10 cm and compacted to fill the spaces. The column was fed from the bottom flowrate of 1.8 mL.min^{-1} by a peristaltic pump. The influent and the effluent were kept constant. The samples were collected from the top of the column. Every 5 mL the samples were analysed and the efficiency of the column system was calculated as shown in Equation 1. In the studies carried out with similar plants, the removal of dyes with concentratıon of 50 ppm from lıquıd solutıon was accomplished in column systems. 50 ppm as initial concentration was accepted and a column study was performed.

3. Result and Discussion

3.1. CS Characterization

In this study, the characterization of the CS adsorbent was carried out to understand the properties of the adsorbent. According to SEM results, the surface of the adsorbent can be considered cruelty, porous and heterogeneous. The SEM was carried to the sample before and after the adsorption process. Figure 3.a shows the raw CS while Figure3.b shows the CS after the adsorption.
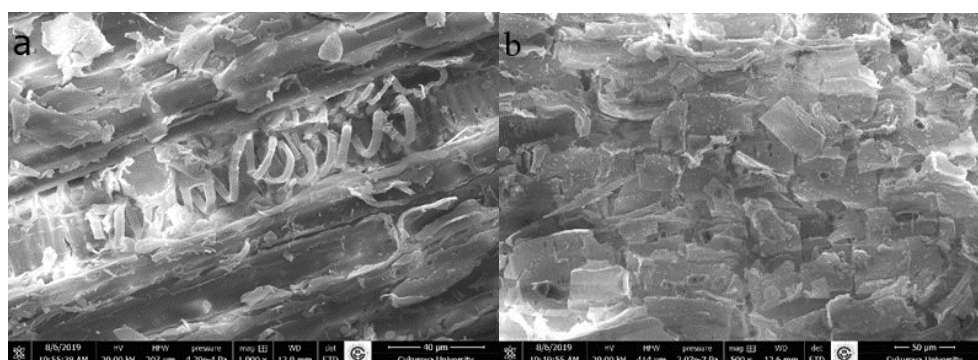

Figure 3. a) SEM for CS before adsorption process b) SEM for CS after adsorption process.

The surface area of the adsorbent CS was measured by BET analysis. The surface area and the Micro pore volume for the adsorbent before the adsorption process were found to be 4.97 $m^2.g^{-1}$ and 0.37 $mm^3.g^{-1}$. This value is 2 times larger than *Xanthium Italicum* (Saleh et al. 2019). The surface area decreased at the end of the adsorption to reach 2.7 $m^2.g^{-1}$. The adsorption process also affected the Micro pore volume since there was no Micro pore detected in the sample.

The Fourier transform infrared spectra for the adsorbent CS was determined using FTIR analysis. The peak related to the functional group of N-H stretching changed from the 3325.64 cm^{-1} to 3276.90 cm^{-1}. The intensity of these peaks increased from 30.45 to 33.14. The intensity of C-H stretching at band 2916.81 cm^{-1} has increased from 24.43 to 29.88. As pointed in Figure 4, the chemical structure of the adsorbent had been changed. Two new peaks were marked. The first peak related to the C-H stretching functional group was noticed at a band of 2849.31 cm^{-1}. The second was at the wavelength of 893.84 cm^{-1} related to the functional group of C-Cl stretching. Three peaks were not noticed after the adsorption process. Those were at the band of 593.97, 1157.08, 1714.41 cm^{-1}.Over the bands from 4000 -400 cm^{-1}, many peaks had been shifted. These results confirm the effect of the functional group. Since the structure of the adsorbent had been changed, the adsorption of MG onto CS can be considered chemisorption.
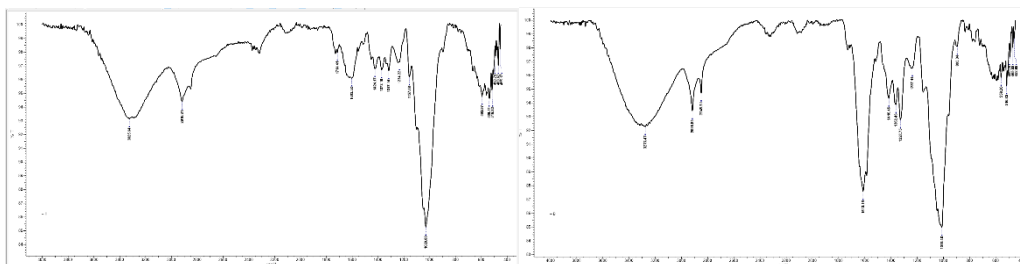

Figure 4. FTIR analysis a) before adsorption b) after adsorption.

3.2. Response Surface Method (RSM)

The batch experiments were designed by RSM. The performance of MG removal from aqueous solutions by CS was modelled (Appendix A shows the experiments and their responses). The four factors effects were studied by Central Composite Design (CCD). The response from the CCD method ranges from 8.14-122.5. The ratio between the maximum and the minimum value was larger than 10, which required a transformation method. The inverse square root transform was selected. Box-Cox graph for power transformation was plotted to compare the current lambda with the best one. Box-Cox plot is shown in Figure 5.
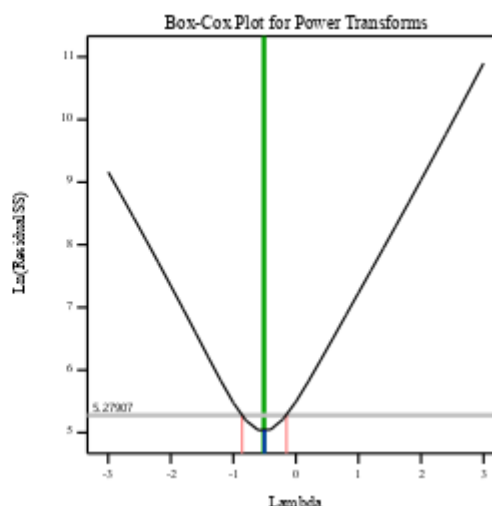

Figure 5. Box-Cox plot for power transformation

The results also were fitted by linear, 2FI, Quadratic and cubic. Since Quadratic has the largest correlation factor, it was chosen to fit the data. Model statistic summary and Sequential Model Sum of Squares are shown in Appendix B.1 and B.2 respectively. Analysis of variance (ANOVA) for the quadratic model was carried out (Appendix B.3). The significant factors were determined via P and F-values. MG removal by CS model was significant since it has an F-value of 68.59. The P-value smaller than 0.01, thus the model is significant at a 99% confidence level (Roosta et al. 2014). In addition to that, the model parameters those have P-value smaller than 0.05 are significant. In this case A, C, D, AC, B², C², D² are significant model terms.

The developed model was used to predict the CS capacity response to the change in the defined parameters. The relationship between the factors and the capacity of the adsorbent is shown in equation 14.

$$\frac{1}{\sqrt{q_t+7}} = 00.331826221 - 0.017824498341752A - 0.00052011920206277B + 0.091813100571215C -$$
$$0.00096958263961297D + 0.00017003283000342AB + 0.014350244234536AC + 0.000013329893732484AD -$$
$$0.00003695009401308BC - 2.7976247962452 \times 10^{-07}BD - 0.00001808374768725CD + 0.0002214615369295A^2 +$$
$$0.000032843042807735B^2 - 0.068342335665863C^2 + 0.0000012792310917991D^2 \qquad \text{Equation 14}$$

Where A, B, C, and D are pH, time (min), mass (g), and concentration (mg.L^{-1}) respectively.

The regression coefficient (R^2) for the created model was found to be 0.9846. The difference between R^2 and the adjusted R^2 was 0.0143, which could be neglected. Same results were obtained by Khamparia and Jaspal (2017). Since the difference between the adjusted R^2 and the predicted R^2 was 0.0589, which is lesser than 0.2. Furthermore, the model showed a good coincidence between the observed and the predicted as shown in Figure 6 (Khamparia and Jaspal 2017).
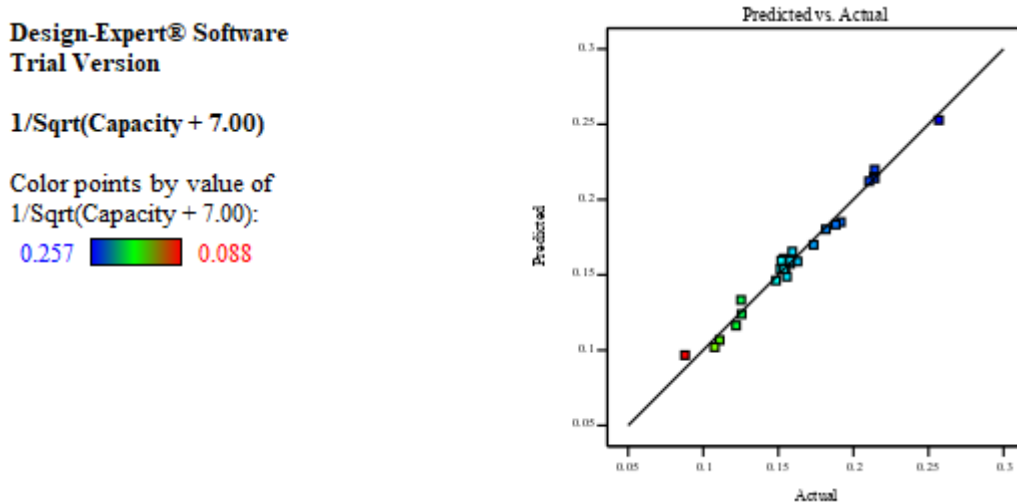

Figure 6. Predicted and the actual results

3.3. Model Optimization

The model was optimized by changing the values of the parameters. The capacity of 90.816 mg.g^{-1} was achieved when MG solution of 312.5 mg.L^{-1} concentration was adsorbed onto 0.325 g CS for 75 min at a pH of 7.5. The desirability of these conditions reached 0.992.

3.4. Effect of Parameters on the Capacity

In this study, the range of pH was between 3 and 9. Because of the bonds between the surface of the CS and the Mg functional group, the CS capacity increases with the pH until pH =7.5. Sartape et al. (2017) used *Limonia acidissima* (wood apple) shell to remove MG from the aqueous solution and the maximum efficiency was when pH ranged between 7.5 and 8. The capacity of the CS has an inverse relationship with the mass of adsorbent. The maximum capacity obtained at 0.325g. Figure 7 shows the relationship between the pH, adsorbent mass and the capacity of CS.
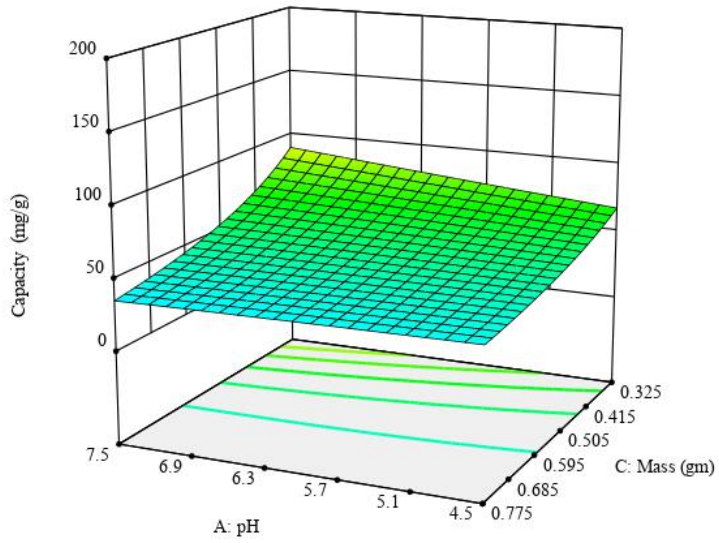
Figure 7. pH, adsorbent mass and the CS capacity relationship at time of 91.25 min and a concentration of 312.5mg.L^{-1}.

The contact time effects were also explored. The capacity increased with time until the minute of 56.75 where it reached the equilibrium and fixed. The concentration of malachite green has a proportional relationship with the capacity as shown in Figure 8. The maximum capacity was found at MG concentration of 312.5 mg.L^{-1}.
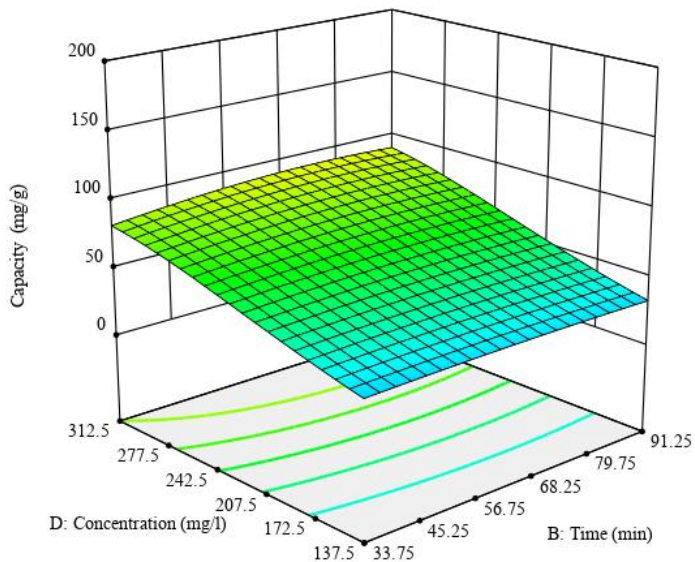

Figure 8. The contact time, MG concentration and the CS capacity relationship at pH = 7.5 and a mass of 0.325 g

3.5. Isotherm

Langmuir, Freundlich, Temkin, and Dubinin-Radushkevich (D-R) isotherms were plotted (as shown in Appendix C). The slope and y-axis intercept were determined to find the isotherms coefficients and summarized in Table 3. Temkin isotherm had the highest

regression value of 0.997, while the Langmuir isotherm had the lowest regression value of 0.697. Temkin isotherm had the best fit than the others. Multi-layers of MG adsorbed onto CS with the heterogeneous surface.

Table 3. Isotherm Coefficient

Isotherm	Coefficient	
Langmuir	$q_m(mg.g^{-1})$	140.85
	$b_A(L.mg^{-1})$	0.008
	R^2	0.697
Freundlich	$1/n$	1.269
	$K_A (mg.g^{-1})(L.mg^{-1})^{1/n}$	0.611
	R^2	0.987
Temkin	$A_T (L. g^{-1})$	-2.40
	b_T	54.57
	R^2	0.997
Dubinin-Radushkevich (D-R)	$K_{ad} (mol^2.KJ^{-2})$	$6*10^{-5}$
	$q_s (mg.g^{-1})$	68.861
	R^2	.988

3.6. Kinetics

Lagergren Pseudo first-order and Pseudo second-order were plotted according to the Equations 8 and 9 as shown in Figures 9 and 10. The correlation factor of the linearity for each one was determined.
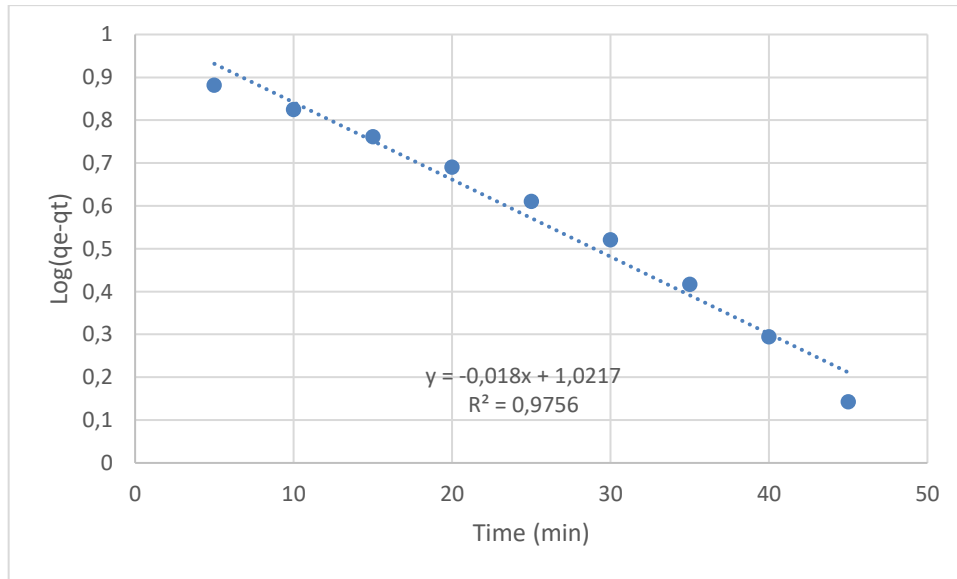

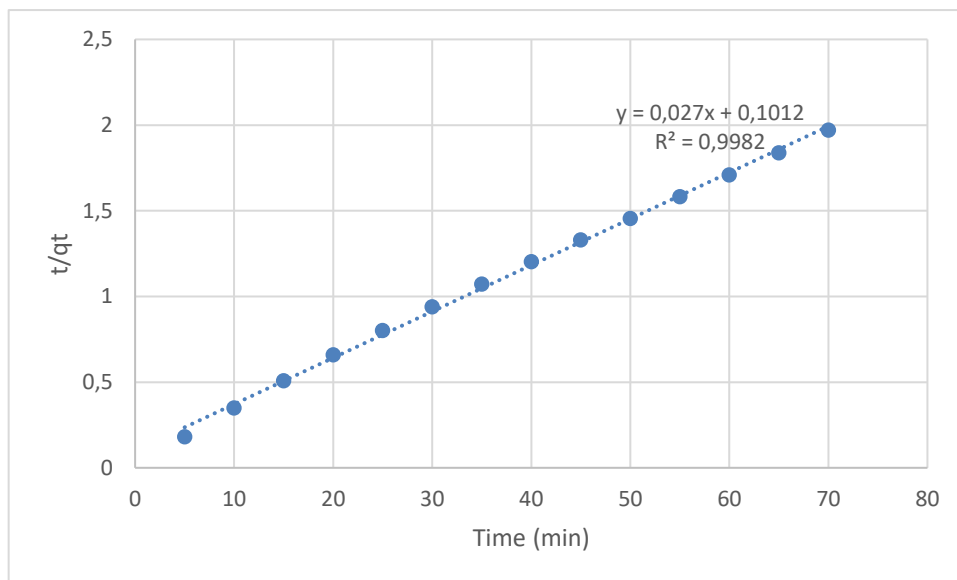*Figure 9. Lagergren's Pseudo-first order*

Figure 10. Pseudo-second order

The adsorption of MG onto CS was fitted to the Pseudo second-order. The correlation factor of the second order was 0.9982, and a rate constant of 0.0072 (gm.g^{-1}.min^{-1}). The first-order kinetic had correlation factor of 0.9756, and a rate constant of 0.04145 min^{-1}. The intraparticle diffusion plots reflected the adsorption steps. It involved two steps; the first linear part comprehended the boundary diffusion layer, while the second portion introduced the intraparticle diffusion effects (Figure11).
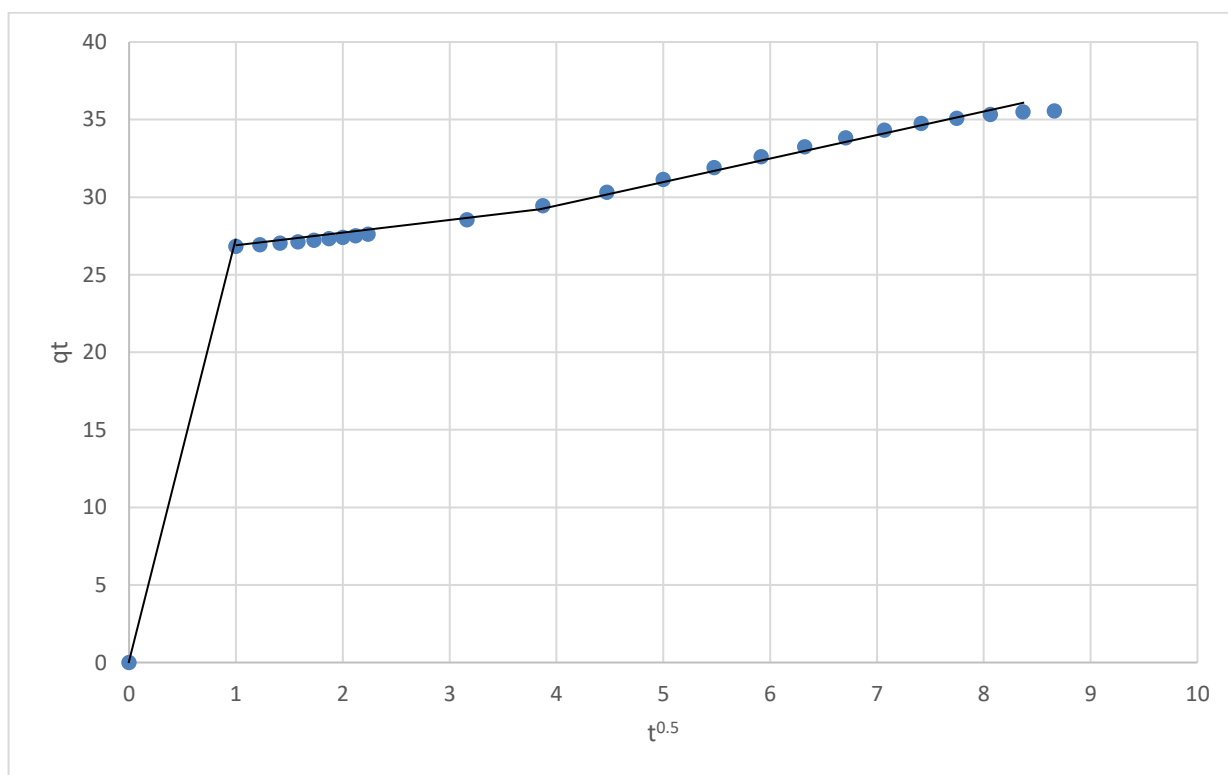

Figure 11. Intraparticle diffusion model for adsorption of MG onto CS.

3.7. Thermodynamics

Adsorption Thermodynamic was identified by the known parameters includes Gibbs free energy, enthalpy, and entropy. The parameters values were summarized as shown in Table 4. The Gibbs energy values for the temperatures 30, 35, 40 were -4.47,-5.66, and -6.46 KJ.mol^{-1} respectively. Although the Gibbs energy located in the range of 0-20KJ.mol^{-1}, the adsorption can be considered chemisorption. The negative sign also showed that the adsorption of MG onto CS was feasible and spontaneous in nature. From the enthalpy, the adsorption was endothermic since it had a positive value. The positive sign of entropy reflected the randomness at the solid phase interface had increased during the adsorption process.

Table 4. Thermodynamic components

Temperature (C)	Temperature(K)	ΔG (KJ.mol⁻¹)	ΔH	ΔS
30	303	-4.47	56.00	0.199
35	308	-5.66		
40	313	-6.46		

3.8. Desorption

Desorption processes were conducted at the end of the adsorption process. The adsorbent was soaked into 0.1M HCL and 0.1 M NaOH solutions separately. It was noted that the adsorption process was irreversible. The max percentage of desorption process was 2.16 % at 180 min in acid batch. After this time, the adsorption process has started again.

3.9. Column Study

As mentioned previously, the column experiments were conducted to realize the adsorption process. A solution of 50 ppm was prepared and pumped from the bottom of the column with a flow of 1.8m L.min⁻¹. The samples were analysed Every 5 mL. The efficiency of the column system was determined as shown in Figure 12. The results show an opportunity to realize the adsorption process of MG onto CS. The first sample reached and collected after 35 min from the pumping process. The efficiency reached 99.5% after 40 min and stilled constant.
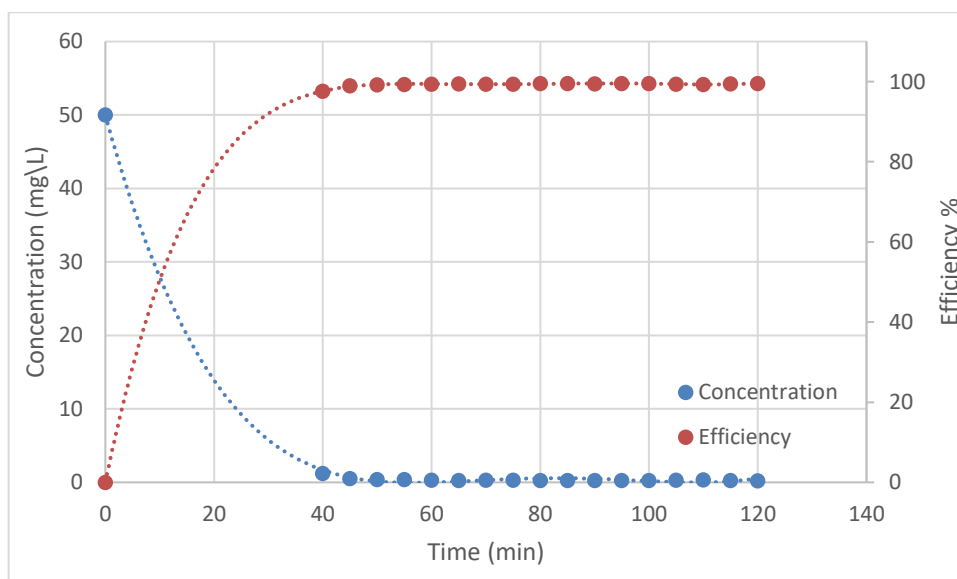

Figure 12. The removal efficiency of MG and the change in concentration along time.

3.10. Previous Studies

Many researchers studied the removal of MG by low cost adsorbent. A comparison between them and proposed adsorbent in this study is shown in Table 5.

Table 5. Comparison between CS and other adsorbent

Adsorbent	Isotherm	Max capacity	Kinetic Model	Thermodynamic	References
Centaurea solstitialis (CS)	Temkin	122.5	Pseudo 2nd order	Endothermic	This study
Almond gum	Langmuir and Freundlich	172.4	Pseudo 2nd order	Endothermic	Bouaziz et al. 2017
Potato stem powder (PSP)	Freundlich	27.6	Pseudo 2nd order	Exothermic	Gupta et al. 2016
Nano chitosan-STP from shrimp shell	Freundlich	317.7	Pseudo 2nd order	-	Salamata et al. 2019
Neem sawdust	Langmuir	4.3	Pseudo 1st order	Endothermic	Khattri and Singh 2009
Walnut shell	Langmuir	90.8	Pseudo 2nd order	Endothermic	Dahri et al. 2014
Rice bran	Freundlich	68.9	Pseudo 2nd order	Spontaneous andphysical	Wang et al. 2008
NaOH-modified breadnut peel	Sips	353	Pseudo 2nd order	Exothermic	Chieng et al. 2015
Mango bark powder (MBP)	Langmuir	0.36 mmo/g	Pseudo 2nd order	Endothermic	(Srivastava & Rupainwar, 2011)
Citric acid (CA) treated pea shells (CAPS)	Freundlich	14,49	Pseudo 2nd order	Endothermic	(Khan, Rahman, Ali, & et.al, 2014)
Limonia acidissima (wood apple) shell	Langmuir	34,56	Pseudo 1st order	Endothermic	(Sartape, Mandhare, Jadhav, & et. al, 2015)
Cellulose modified with phthalic (P) anhydride (CPA)	Langmuir	111	Pseudo 2nd order	Endothermic	(Zhou et al, 2015)

4. Conclusion

In this study, invasive CS plant which is agricultural waste was used as adsorbent for removal of MG from aqueous solution. The experiments were designed and modelled by RSM. The correlation factor of the developed model was 0.984. Temkin isotherm had the highest R^2 of 0.997. The kinetics models of the adsorption process were investigated and found to be fit with pseudo-second-order kinetic (R^2=0.9982). The intraparticle diffusion model reflected the involved two steps; the first comprehended the boundary diffusion layer, while the second introduced the intraparticle diffusion effects. The adsorption was found to be endothermic. Although the Gibbs energy located in the range of 0-20 KJ.mol^{-1}, the adsorption can be considered chemisorption. It was noted that the adsorption process was irreversible with a max percentage of desorption process of 2.16%. Column experiment realized the adsorption process. The efficiency of the column reached 99.5% after 40 min and stilled constant.

Centaurea solstitialis (CS) was used successfully in adsorption of the Malachite Green dye. Reducing or eliminating the negative environmental impact of dye-containing wastewater is of great importance for the textile industry today. Chemical treatment is the most effective and common method used for removing dyes from wastewater. Due to the chemical content of the generated sludge from the treatment system, the development of more environmentally friendly technologies is an important research topic today. Adsorption is another effective dye removal process. One of the most important problems in this process is the elimination of the dye-filled adsorbent. One of the most important features of using plant origin materials as adsorbents is that the plant does not allow the adsorbed dyes to return to the water. In this study, the dye desorption of the CS plant was found to be very low. Also, the environment can be inoperative by adsorbent after the adsorption process by burning plant wastes in emission controlled industrial facilities. The used CS in this study is an invasive plant. After the removal of invasive plants from the agricultural fields, they are left to rot or burn around the field. Emissions from uncontrolled combustion in the open area contribute to air pollution. There is no use of CS as animal feed.

5. Acknowledge

Kaynakça

Abd-El-Kareem, M., & Taha, H. (2012). Decolorization of malachite green and methylene blue by two microalgal species. *Int J Chem Environ*, 3, 297-302.

Aharoni, C., & Ungarish, M. (1977). Kinetics of activated chemisorption. Part 2. Theoretical models. *J. Chem. Soc. Faraday Trans.*, 73, 456–464.

Aliyan, H., Fazaeli, R., & Jalilian, R. (2013). Fe3O4 at mesoporous SBA-15: a magnetically recoverable catalyst for photodegradation of. *Appl Surf Sci*, 276, 147–153. doi:10.1016/j.apsusc.2013.03.049

Bagheri, A. R., Arabi, M., Ghaedi, M., Ostovan, A., Wang, X., Li, J., & Chen, L. (2019). Dummy molecularly imprinted polymers based on a green synthesis strategy for magnetic solid-phase extraction of acrylamide in food samples. *Talanta,* 195, 390-400.

Bai, C., Xiao, W., Feng, D., & al, e. (2013). Efficient decolorization of Malachite Green in the Fenton reaction catalyzed by [Fe (III)-salen] Cl complex. *Chem Eng J,* 215-216, 227-234. doi:10.1016/j.cej.2012.09.124

Bapat, S., & Jaspal, D. (2016). Parthenium hysterophorus: novel adsorbent for the removal of heavy metals and dyes. *Glob. J. Environ. Sci. Manag.*, 2, 135-144. doi:http://dx.doi.org/10.7508/gjesm.2016.02.004.

Belhouchat, N., Zaghouane-Boudiaf, H., & Viseras, C. (2017). Removal of anionic and cationic dyes from aqueous solution with activated organo-bentonite/sodium alginate encapsulated beads. *Appl. Clay Sci*, 135, 9-15.

Bezerraa, M. A., Santelli, R. E., Oliveira, E. P., Villar, L. S., Ame, L., & Escaleira, l. (2008). Response surface methodology (RSM) as a tool for optimization in analytical chemistry. *Talanta*, 76, 965-977.

Bojinova, A., & Dushkin, C. (2011). Photodegradation of malachite green in water solutions by means of thin films of TiO2/WO3 under visible light. *React Kinet Mech Catal*, 103, 239–250. Doi: 10.1007/s11144-011-0295-2

Bouaziz, F., Koubaa, M., Kallel, F., Ghorbel, R. E., & Chaabouni, S. E. (2017). Adsorptive removal of malachite green from aqueous solutions by almond gum: Kinetic study and equilibrium isotherms. *International Journal of Biological Macromolecules*, 105, 56-65.

Chen, F., Ma, W., He, J., & Zhao, J. (2002). Fenton degradation of malachite green catalyzed by aromatic additives. *J Phys Chem A*, 106, 9485–9490. Doi: 10.1021/jp0144350

Chieng, H., Lim, L., & Priyantha, N. (2015). Enhancing adsorption capacity of toxic malachite green dye through chemically modified breadnut peel: equilibrium, thermodynamics, kinetics and regeneration studies. *Environ Technol*, 36, 86-97.

Crittenden, J. C., Trussell, R. R., Hand, D. W., Howe, K. J., & Tchobanoglous, G. (2012). *MWH's Water Treatment Principles and Design (Third Edition Ed.)*. New Jersey: John Wiley & Sons, Inc.

Dabrowski, A. (2001). Adsorption—from theory to practice. Adv. Colloid Interface Sci., 93, 135–224.

Dahri, M. K., Kooh, M. R., & Lim, L. B. (2014). Water remediation using low cost adsorbent walnut shell for removal of malachite green: Equilibrium, kinetics, thermodynamic and regeneration studies. *Journal of Environmental Chemical Engineering*, 2, 1434-1444.

Freundlich, H. (1906). Over the adsorption in solution. *J. Phys.Chem.*, 57, 385-470.

Gadekar, M. R., & Ahammed, M. M. (2019). Modelling dye removal by adsorption onto water treatment residuals using combined response surface methodology-artificial neural network approach. *J. Environ. Manag.* 231, 241-248.

Gunay, A., Arslankaya, E., & Tosun, I. (2007). Lead removal from aqueous solution by natural and pretreated clinoptilolite: adsorption equilibrium and kinetics. *J.Hazard. Mater*, 146, 362–371.

Gupta, N., Kushwaha, A. K., & Chattopadhyaya, M. (2016). Application of potato (Solanumtuberosum) plantwastes for the removal of methylene blue and malachite green dye form aqueous solution. *Arabian Journal of Chemistry* (9), 707-716. Retrieved from https://doi.org/10.1016/j.arabjc.2011.07.021

Gupta, V. (2009). Application of low-cost adsorbents for dye removal- A review. *J. Environ. Manag*. 90, 2313-2342.

Gupta, V. K., Nayak, A., & Agarwal, S. (2015). Bioadsorbents for remediation of heavy metals: current status and their future prospects. *Environ. Eng. Res.*, 1(20), 1-18.

Hasnat, M., Siddiquey, I., & Saiful, I. (2003). Photodegradation of malachite green in the aqueous medium. *Indian J Chem Sect A*, 42, 1865–1867.

Khamparia, S., & Jaspal, D. K. (2017). Xanthium strumarium L. seed hull as a zero cost alternative for Rhodamine B dye removal. *J. Environ. Manag*. 197, 498-506.

Khan, T., Sharma, S., & Ali, I. (2011). Adsorption of Rhodamine B dye from aqueous solution onto acid activated mango (Magnifera indica) leaf powder: equilibrium. *J. Toxicol. Env. Health Sci.*, 3, 286-297.

Khattri, S., & Singh, M. (2009). Removal of malachite green from dye wastewater using neem sawdust by adsorption. *J Hazard Mater,* (167), 1089-1094. Retrieved from https://doi.org/10.1016/j.jhazmat.2009.01.101

Langmuir, I. (1918). The adsorption of gases on plane surfaces of glass, mica and platinum. . *Am. Chem. Soc.,* 40, 1361-1403.

Levin, L., Papinutti, L., & Forchiassin, F. (2004). Evaluation of Argentinean white rot fungi for their ability to produce lignin-modifying enzymes and decolorize industrial dyes. *Bioresour Technol,* 94, 169–176. doi:10.1016/j.biortech.2003.12.002

Man, L., Kumar, P., Teng, T., & Wasewar, K. (2012). Design of experiments for malachite green dye removal from wastewater using thermolysis—coagulation–flocculation. *Desalin Water Treat,* 40, 260-271. doi:10.1080/19443994.2012.671257

Mittal, A., Mittal, J., Malviya, A., & Gupta, V. (2009). Adsorptive removal of hazardous anionic dye "Congo Red" from wastewater using waste materials and recovery by desorption. *J. Colloid Interface,* 340, 16-26. doi:10.1016/j.jcis.2009.08.019

Modirshahla, N., & Behnajady, M. (2006). Hot oxidative degradation of malachite green (MG) by UV/H2O2: influence of operational parameters and kinetic modelling. *Dyes Pigments*, 70, 54-59. doi:10.1016/j.dyepig.2005.04.012

Pal, P., & Pal, A. (2017). Surfactant-modified chitosan beads for cadmium ion adsorption. *Int. J.Biol. Macromol.* 104, 1548-1555.

Pirsaheb, M., Shahmoradi, B., Khosravi, T., & al, e. (2015). Solar degradation of malachite green using nickel-doped TiO2 nanocatalysts. *Desalin Water Treat*, 57, 9881–9888. doi:10.1080/19443994.2015.1033764

Raval, N., Shah, P., & Shah, N. (2016). Nanoparticles loaded biopolymer as effective adsorbent for adsorptive removal of malachite green from aqueous solution. *Water Conserv Sci Eng,* 1, 69-81. Doi: 10.1007/s41101-016-0004-0

Robati, D. (2013). Pseudo-second-order kinetic equations for modeling adsorption systems for removal of lead ions using multi-walled carbon nanotube. *J. Nanostructure Chem.*, 3(55).

Robinson, T., McMullan, G., Marchant, R., & Nigam, P. (2001). Remediation of dyes in textile effluent: a critical review on current treatment technologies with a proposed alternative. Bioresour. *Technol.,* 77, 247-255. doi:http://dx.doi.org/10.1016/S0960-8524 (00)00080-8.

Roosta, M., Ghaedi, M., Shokri, N., Daneshfar, A., Sahraei, R., & Asghari, A. (2014). Optimization of the combined ultrasonic assisted/adsorption method for the removal of malachite green by gold nanoparticles loaded on activated carbon: experimental design. *Spectrochimica Acta Part A Mol. Biomol. Spectrosc.* 118, 55-65.

Sartape, S.A., Mandhare, A. M., Jadhav, V. V., Raut, P. D., Anuse, M. A., & Kolekar, S. S. (2017). Removal of malachite green dye from aqueous solution with adsorption technique using Limonia acidissima (wood apple) shell as low cost adsorbent. *Arabian Journal of Chemistry*, 10, S3229-S3238.

Salamata, S., Hadavifar, M., & Rezaei, H. (2019). Preparation of nanochitosan-STP from shrimp shell and its application in removing of malachite green from aqueous solutions. *Journal ofEnvironmental Chemical Engineering*, 7. doi:https://doi.org/10.1016/j.jece.2019.103328

Saleh, M., Yalvaç, M., & Arslan, H. (2019). Optimization of Remazol Brilliant Blue R Adsorption onto Xanthium Italicum using the Response Surface Method. *Karbala International Journal of Modern Science*, 5(1). doi:10.33640/2405-609X.1017

Salleh, M. A., Mahmoud, D. K., Karim, W. A., & Idris, A. (2011). Cationic and anionic dye adsorption by agricultural solid wastes: A comprehensive review. *Desalination* (280), 1-13. Retrieved from http://dx.doi.org/10.1016/j.desal.2011.07.019

Saravanan, R., Sacari, E., Gracia, F., Khan, M., Mosquera, E., & Gupta, V. (2016). Conducting PANI stimulated ZnO system for visible light photocatalytic degradation of coloured dyes. *Journal of Molecular Liquids*, 221, 1029-1033. doi:10.1016/j.molliq.2016.06.074

Sartepe, A. S., Mandhare, A. M., Jadjav, V. V., Raut, P. D., Anuse, M. A., & Kolekar, S. S. (2017). Removal of malachite green dye from aqueous solution with adsorption technique using Limonia acidissima (wood apple) shell as low cost adsorbent. *Arabian Journal of Chemistry* (10), 3229-3238. Retrieved from https://doi.org/10.1016/j.arabjc.2013.12.019

Saxena, S., & Raja, A. (2014). *Natural Dyes: Sources, Chemistry, Application and Sustainability Issues*. In Muthu S. (Eds) Roadmap to Sustainable Textiles and Clothing (pp. 37-80). Singapore: Textile Science and Clothing Technology. Springer.

Tempkin, M., & Pyzhev, V. (1940). Kinetics of ammonia synthesis on promoted iron catalyst. *Acta Phys. Chim*, USSR 12, 327–356.

Tobías, S., Ignacio, D., Lorena, A., Gustavo, P., Matías, L., Isabela, O., Sebastian, B. (2018). Design and testing of a pilot scale magnetic separator for the treatment of textile dyeing wastewater. *J. Environ. Manag.* 218, 562-568.

TÜİK, T. (2018). Paint Industry in Turkey and the World. Paint Istanbul& Turkcoat 2018. Istanbul. Retrieved 08 19, 2019, from http://www.turkcoat-paintistanbul.com/uploads/files/Paintistanbul_Turkcoat_2018_Preview.pdf

Wang, X., Zhou, Y., Jiang, Y., & Sun, C. (2008). The removal of basic dyes from aqueous solutions using agricultural by-products. *J Hazard Mater*, 157, 374-385.

Yang, J., Chen, C., Ji, H., & al, e. (2005). Mechanism of TiO2-assisted photocatalytic degradation of dyes under visible irradiation: photoelectrocatalytic study by TiO2-film electrodes. *J Phys Chem B*, 109, 21900–21907. Doi: 10.1021/jp0540914

Zhou, X.-J., Guo, W.-Q., Yang, S.-S., & al, e. (2013). Ultrasonic-assisted ozone oxidation process of triphenylmethane dye degradation: evidence for the promotion effects of ultrasonic on malachite green decolorization and degradation mechanism. *Bioresour Technol*, 128, 827-830. doi:10.1016/j.biortech.2012.10.086

Khan, T., Rahman, R., Ali, I., & et.al. (2014). Removal of malachite green from aqueous solution using waste pea shells as low-cost adsorbent—adsorption isotherms and dynamics. *Toxicol Environ Chem, 96*, 569-578. doi:10.1080/02772248.2014.969268

Sartape, A., Mandhare, A., Jadhav, V., & et. al. (2015). Removal of malachite green dye from aqueous solution with adsorption technique using Limonia acidissima (wood apple) shell as low cost adsorbent. *Arab J Chem.* doi:10.1016/j.arabjc.2013.12.019

Srivastava, R., & Rupainwar, D. (2011). A comparative evaluation for adsorption of dye on Neem bark and Mango bark powder. *Indian J Technol, 18*, 67-75.

Zhou, Y., Min, Y., Qiao, H., & et. al. (2015). Improved removal of malachite green from aqueous solution using chemically modified cellulose by anhydride. *Int J Biol Macromol, 74*, 271-277. doi:10.1016/j.ijbiomac.2014.12.020